Journal of Quantitative Spectroscopy & Radiative Transfer ▮ (▮▮▮▮) ▮▮▮–▮▮▮

Contents lists available at SciVerse ScienceDirect

Journal of Quantitative Spectroscopy & Radiative Transfer

journal homepage: www.elsevier.com/locate/jqsrt

Re-analysis of the (100), (001), and (020) rotational structure of SO_2 on the basis of high resolution FTIR spectra

O.N. Ulenikov [a,*], G.A. Onopenko [b], O.V. Gromova [a,c], E.S. Bekhtereva [a], V.-M. Horneman [d]

[a] Laboratory of Molecular Spectroscopy, Physics Department, National Research Tomsk State University, Lenin av., 36, 634050 Tomsk, Russia
[b] Department of Applied Mathematics, Tomsk University of Architecture and Building, Tomsk 634003, Russia
[c] Department of Theoretical and Experimental Physics, Institute of Physics and Technology, National Research Tomsk Polytechnic University, Tomsk 634050, Russia
[d] Department of Physics, University of Oulu, P.O. Box 3000, FIN-90014, Finland

ARTICLE INFO

Article history:
Received 28 February 2013
Received in revised form
7 April 2013
Accepted 8 April 2013

Keywords:
Sulfur dioxide
Ground state
High-resolution spectra
Spectroscopic parameters
$\nu_1/2\nu_2/\nu_3$ bands

ABSTRACT

Three infrared spectra, weak (W), medium (M), and strong (S), of the $^{32}SO_2$ molecule were recorded with high resolution in the 1000–1500 cm^{-1} region. Spectra were recorded with the Fourier Transform interferometer Bruker IFS-120 HR in Oulu (Finland) with different pressures, absorption path lengths, and recording time. That allowed us to record not only the ν_1 and ν_3 bands with higher values of quantum numbers J and K_a than it was made earlier, but to record for the first time very weak $2\nu_2$ band. In this case, transitions with the values $J^{max.}/K_a^{max.}$ equal to 89/37, 109/28, and 54/9 were assigned in the experimental spectra for the bands ν_1, ν_3, and $2\nu_2$, respectively. As it became clear in the course of the analysis, the rotational parameters of the ground vibrational state, known in the literature, do not describe suitably the ground state combination differences (GSCD) for the states with the value $K_a > 26$–27. As a consequence, the ground state rotational parameters were improved on the basis of our experimental data. The 12 131 transitions assigned in the experimental spectrum (7618, 3952, and 561 transitions of the bands ν_1, ν_3, and $2\nu_2$, respectively) were used for determination of ro-vibrational energy values of the vibrational states (100), (001), and (020). The lasts were used then in the fit procedure together with known in the literature high accurate sub-millimeter wave data. Resonance interactions between all three vibrational states have been taken into account in the Hamiltonian used for the fit. As a result, the 51 varied parameters, obtained from the fit, reproduce 4063 ro-vibrational energies of the states (100), (001), and (020) (12 131 initial experimental transitions) with accuracies close to experimental uncertainties: the rms deviation is 6.1×10^{-5} cm^{-1}, 9.7×10^{-5} cm^{-1}, and 13.9×10^{-5} cm^{-1} for our FTIR data (for the (100), (001), and (020) states, respectively), and comparable with experimental uncertainties for heterodyne data.

1. Introduction

Sulfur dioxide is an important chemical species in many fields such as chemistry, astrophysics, laser techniques. It plays an important role as a pollutant in the terrestrial atmosphere. In particular, sulfur dioxide is one of the major air pollutants released in the atmosphere as a result of volcanic eruptions and of fuel combustion in human activities; it contributes to the generation of smog and constitutes a serious health hazard for the respiratory system. To solve the problems of propagation of monochromatic radiation in the atmosphere, laser sounding, information transfer,

* Corresponding author. Tel.: +7 962 785 9656.
E-mail address: ulenikov@phys.tsu.ru (O.N. Ulenikov).

0022-4073/$ - see front matter © 2013 Elsevier Ltd. All rights reserved.
http://dx.doi.org/10.1016/j.jqsrt.2013.04.011

the remote detection and monitoring of SO_2 in situ, etc., one also should have a good knowledge of the fine structure of the SO_2 absorption spectra in different parts of the electromagnetic spectrum, in particular, in the infrared. Therefore, spectroscopic studies of the sulfur dioxide molecule have been made during many years both in the microwave, and sub-millimeter wave and infrared regions (see, Refs. [1–35].

In this paper we follow up on our recent studies of the high resolution spectra of SO_2, Refs. [36–40]. The subject of the present study is the region of 1000–1500 cm^{-1}. This region, where the strongest SO_2 ν_3 and ν_1 bands, and very weak $2\nu_2$ band are located, is ideal for infrared atmospheric measurements of that molecule. Earlier the ν_1 and ν_3 bands were discussed in Refs. [5,12,16,21,23]. All information containing in these references were then generalized in Ref. [26]. But the information about the band $2\nu_2$ was absent, and ro-vibrational energies of the (020) state were determined from the hot $2\nu_2$–ν_2 band [21]. In our present analysis, we were able to assign transitions of the ν_1 and ν_3 bands with values of quantum numbers J and K_a considerably higher than in Ref. [26]. Moreover, transitions of the very weak $2\nu_2$ band also were recorded and assigned for the first time. Section 2 describes the experimental conditions for the recording spectra. In Section 3 we briefly present the Hamiltonian model used to fit the experimental line positions. Description of the spectra, assignment of transitions, and the problem of improvement of the ground state rotational parameters are discussed in Section 4. The results of analysis of the high resolution spectra of the bands ν_1, ν_3 and $2\nu_2$ and determination of spectroscopic parameters of the states (100), (001), and (020) are presented in Section 5.

2. Experimental details

For this molecular research three infrared spectra (weak, medium, and strong) of the $^{32}SO_2$ molecule in the region from 1000 to 1500 cm^{-1} were recorded with a high resolution Fourier Transform spectrometer Bruker IFS-120 HR in the infrared laboratory at the University of Oulu (Finland). In these measurements two absorption cells were used. In the W and M registrations the SO_2 sample, made by Sigma-Aldrich Inc., was introduced in a White type cell, Ref. [41], at the pressure of 11.7 and 110.7 Pa, respectively. The absorption path length (APL) was 3.2 m. In the S measurement the sample was at pressure of 110.7 Pa in another cell, Ref. [42], with APL=163.2 m. The both cells have been optimized for the used spectrometer, and they were provided with potassium bromide (KBr) windows in these measurements. The instrumental resolution at 1100 cm^{-1} was better than 0.0019 cm^{-1} in all three registrations. A globar source, a germanium film between two KBr plates, as the beamsplitter, and mercury cadmium telluride (MCT) detector were used. The registration times were 42.4, 79.9 and 99.9 h in the W, M and S measurements, respectively. The spectra were calibrated with peaks of the OCS $2\nu_2$ band [43] measured in fourth registration together with the sample spectrum. The peak positions were calculated with an optimized center of gravity method [44].

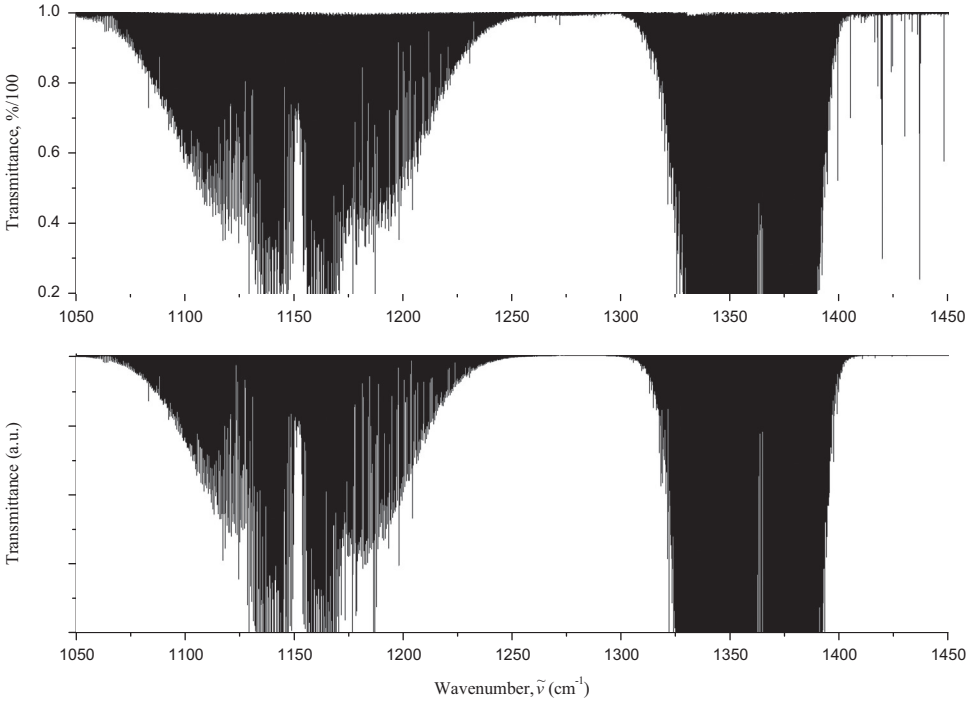

Fig. 1. Survey weak (W) spectrum of SO_2 in the region of 1050–1450 cm^{-1}. Experimentally recorded strong bands ν_1 and ν_3 can be seen in the upper part of the figure. Experimental conditions: absorption path length is 3.2 m; sample pressure is 11.7 Pa; room temperature; registration times is 42.4 h. Synthetic spectrum is shown on the lower part of the figure. In the 1400–1450 cm^{-1} spectral range, some lines that are appeared in the experimental spectrum but not in the calculated one, belong to H_2O.

Please cite this article as: Ulenikov ON, et al. Re-analysis of the (100), (001), and (020) rotational structure of SO_2 on the basis of high resolution FTIR spectra. J Quant Spectrosc Radiat Transfer (2013), http://dx.doi.org/10.1016/j.jqsrt.2013.04.011

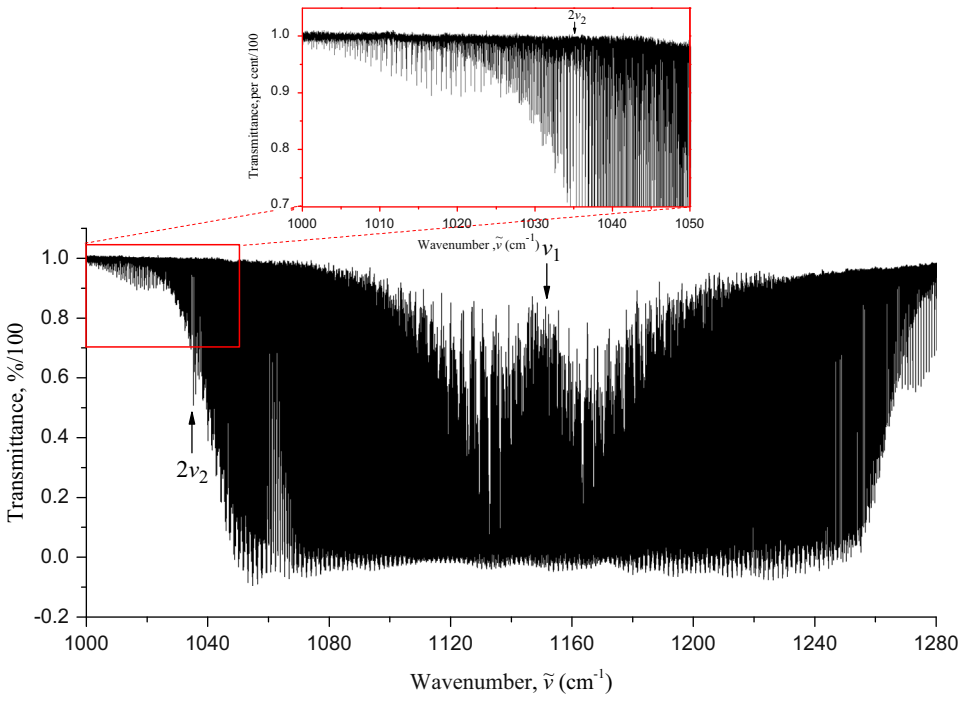

Fig. 2. Survey strong (S) spectrum of SO_2 in the region of the ν_1 and $2\nu_2$ bands. The P-branch of the weak $2\nu_2$ band is seen in the left part of the figure. Experimental conditions: absorption path length is 163.2 m; sample pressure is 110.7 Pa; room temperature; registration times is 99.9 h.

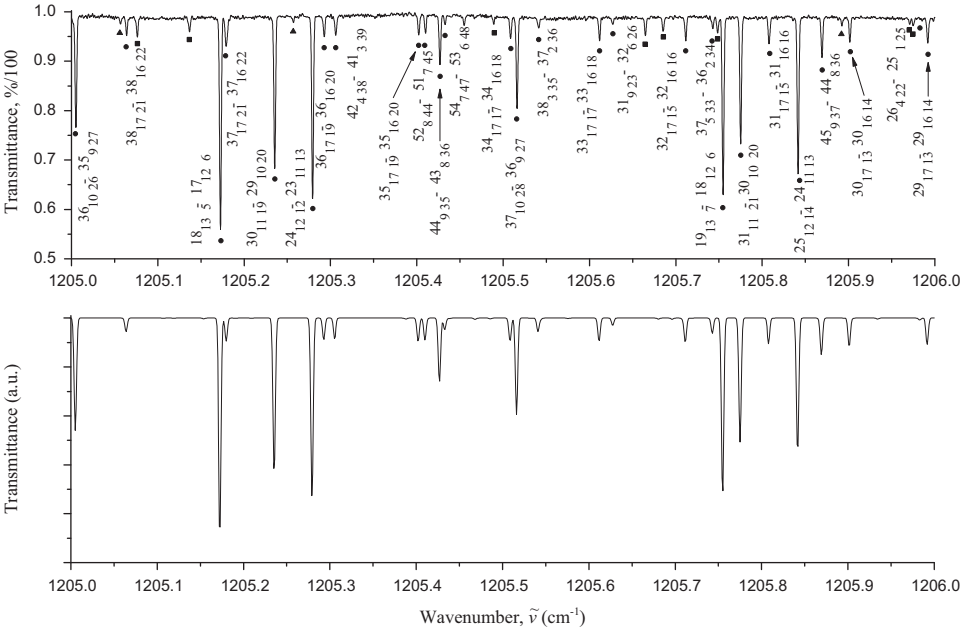

Fig. 3. A small part of the high resolution spectrum of SO_2 in the region of *R*-branch of the ν_1 band (upper part). Experimental conditions correspond to the weak spectrum W. Lines of $^{32}SO_2$ are marked by dark circle. Some weak lines which are absent in the synthetic spectrum (lower part), belong to the hot band $\nu_1+\nu_2$ (they are marked by dark square), or to the $^{34}SO_2$ isotopic species (they are marked by dark triangle).

3. Hamiltonian model

The SO_2 molecule is an asymmetric top of the C_{2v} symmetry. On this reason its three vibrational modes possess the following symmetry: $q_\lambda \in A_1$ for $\lambda=1,2$, and $q_\lambda \in B_1$ for $\lambda=3$. As a consequence, two type bands are allowed in absorption: parallel (or A_1) type bands that correspond to the vibrational transitions $(\nu_{A_1})\leftarrow(\nu_{gr.})$ and perpendicular (or B_1) type bands that correspond to the vibrational transitions $(\nu_{B_1})\leftarrow(\nu_{gr.})$. The selection rules for

Please cite this article as: Ulenikov ON, et al. Re-analysis of the (100), (001), and (020) rotational structure of SO_2 on the basis of high resolution FTIR spectra. J Quant Spectrosc Radiat Transfer (2013), http://dx.doi.org/10.1016/j.jqsrt.2013.04.011

Table 1
High accurate sub-millimeter wave transitions of the SO_2 molecule.

Transition 1							Frequency, exp.[a] in MHz 2	Δ (calc)[b] in kHz 3	Δ (calc)[c] in kHz 4
70	8	62	←	70	7	63	492 056.427(10)	0.3	2.2
68	8	60	←	68	7	61	496 010.525(15)	−1.0	4.4
69	8	62	←	68	9	59	498 109.421(20)	−16.2	−5.1
49	15	35	←	50	14	36	498 657.914(10)	−7.0	2.5
70	9	61	←	69	10	60	498 920.109(20)	8.0	5.3
72	8	64	←	72	7	65	499 505.309(10)	0.9	−0.6
54	16	38	←	55	15	41	500 111.014(10)	1.5	1.9
59	17	43	←	60	16	44	501 179.560(15)	10.0	4.6
64	18	46	←	65	17	49	501 871.632(20)	16.1	4.2
53	16	38	←	54	15	39	519 365.544(10)	−0.5	2.0
58	17	41	←	59	16	44	520 382.480(15)	3.8	1.6
63	18	46	←	64	17	47	521 011.924(20)	15.4	8.6
73	20	54	←	74	19	55	521 137.011(100)	42.9	−10.3
68	19	49	←	69	18	52	521 261.295(40)	15.4	−4.0
47	15	33	←	48	14	34	537 227.581(10)	−11.9	1.2
52	16	36	←	53	15	39	538 602.765(10)	−3.4	1.3
77	7	71	←	78	4	74	539 061.368(60)	−13.6	21.8
57	17	41	←	58	16	42	539 570.174(10)	2.4	3.0
78	6	72	←	79	5	75	539 807.786(100)	−9.2	22.4
72	20	52	←	73	19	55	540 112.736(40)	34.9	−3.8
62	18	44	←	63	17	47	540 139.119(20)	9.6	7.0
75	9	67	←	74	10	64	543 973.462(10)	−11.9	−6.3
80	9	71	←	80	8	72	548 752.732(20)	−15.6	−8.7
76	8	68	←	76	7	69	549 848.964(10)	−1.4	−9.7
78	9	69	←	78	8	70	551 403.734(40)	13.3	22.8
41	7	35	←	42	4	38	564 029.767(15)	−28.2	2.5
51	8	44	←	52	5	47	564 469.319(10)	−20.6	6.4
72	9	63	←	71	10	62	564 665.735(10)	10.0	2.0
76	9	67	←	76	8	68	564 896.451(20)	−9.0	2.2
60	4	56	←	61	3	59	567 304.250(20)	8.9	−1.8
70	7	63	←	70	6	64	569 387.048(10)	6.3	−6.9
69	6	64	←	70	3	67	571 153.962(20)	−7.3	−6.8
51	4	48	←	52	1	51	574 052.463(10)	6.1	1.2
50	16	34	←	51	15	37	577 028.807(10)	−9.6	−1.4
79	7	73	←	80	4	76	577 256.699(60)	14.7	56.4
55	17	39	←	56	16	40	577 902.912(10)	−2.5	2.6
70	20	50	←	71	19	53	578 039.819(30)	1.9	−13.8
60	18	42	←	61	17	45	578 356.855(15)	−4.6	−0.1
65	19	47	←	66	18	48	578 399.767(20)	−22.9	−22.1
70	5	65	←	71	4	68	579 237.260(20)	−1.9	−0.8
84	9	75	←	84	8	76	579 739.581(30)	8.6	9.1

Please cite this article as: Ulenikov ON, et al. Re-analysis of the (100), (001), and (020) rotational structure of SO_2 on the basis of high resolution FTIR spectra. J Quant Spectrosc Radiat Transfer (2013), http://dx.doi.org/10.1016/j.jqsrt.2013.04.011

43	3	41	←	44	0	44	580 618.830(15)	−2.7	0.5
66	8	58	←	65	9	57	582 021.341(10)	7.4	−3.1
74	9	65	←	74	8	66	587 316.386(10)	−9.4	3.3
52	3	49	←	53	2	52	587 329.413(20)	−2.1	−6.6
60	8	52	←	60	7	53	589 642.638(20)	−11.4	5.3
78	8	70	←	78	7	71	591 273.845(20)	−4.3	−15.1
87	9	79	←	86	10	76	594 696.788(150)	−43.3	−87.2
61	5	57	←	62	2	60	595 211.514(15)	6.2	−3.3
74	21	53	←	75	20	56	596 152.773(40)	15.8	−21.9
69	20	50	←	70	19	51	596 992.147(15)	−1.9	−8.7
54	17	37	←	55	16	40	597 049.441(10)	−6.2	0.6
59	18	42	←	60	17	43	597 448.686(15)	−5.3	1.7
87	11	77	←	86	12	74	598 308.577(100)	−31.9	33.3
79	9	71	←	78	10	68	598 780.232(40)	3.9	0.2
64	6	58	←	64	5	59	598 870.113(10)	11.7	−0.9
90	10	80	←	90	9	81	604 987.346(50)	−17.1	−4.8
88	10	78	←	88	9	79	606 878.473(30)	4.0	16.4
71	6	66	←	72	3	69	608 950.898(15)	−8.6	−3.9
53	4	50	←	54	1	53	610 672.068(20)	5.9	1.6
86	9	77	←	86	8	78	613 196.700(15)	7.7	4.4
78	22	56	←	79	21	59	613 688.670(100)	23.0	−38.6
85	9	77	←	84	10	74	613 832.775(40)	55.0	24.3
83	10	74	←	82	11	71	614 447.635(60)	8.6	17.1
81	9	73	←	80	10	70	614 502.717(40)	10.7	−0.4
73	21	53	←	74	20	54	615 016.345(50)	−1.1	−25.2
92	10	82	←	92	9	83	615 483.758(80)	−12.5	0.1
50	2	48	←	51	1	51	706 704.602(20)	−12.2	−3.9
67	5	63	←	68	2	66	706 913.649(40)	−5.8	−10.9
73	22	52	←	74	21	53	707 518.795(60)	−12.2	−6.4
90	9	81	←	90	8	82	709 401.348(50)	45.4	35.3
59	4	56	←	60	1	59	720 632.005(10)	5.7	4.5
77	6	72	←	78	3	75	722 301.996(60)	4.5	11.2
77	23	55	←	78	22	56	723 997.268(100)	−43.8	3.4
51	3	49	←	52	0	52	725 315.755(15)	−0.1	9.1
67	21	47	←	68	20	48	728 114.583(20)	−24.2	−12.3
92	11	81	←	92	10	82	730 959.918(80)	7.4	−30.3
60	3	57	←	61	2	60	738 134.248(15)	−0.6	−1.4
77	11	67	←	78	8	70	738 260.372(150)	1.8	10.6
90	11	79	←	89	12	78	738 649.459(120)	18.6	62.7
78	5	73	←	79	4	76	739 107.558(30)	30.9	33.5
52	2	50	←	53	1	53	743 042.148(20)	−8.3	2.0
69	5	65	←	70	2	68	743 967.302(20)	−4.6	−10.3
71	22	50	←	72	21	51	745 040.392(50)	−9.8	2.3
61	4	58	←	62	1	61	757 135.303(20)	−1.0	−1.6
79	6	74	←	80	3	77	759 786.331(50)	−9.0	−9.3
75	23	53	←	76	22	54	761 344.940(100)	−11.4	43.3
70	4	66	←	71	3	69	761 438.989(30)	−5.5	−12.4
70	22	48	←	71	21	51	763 800.214(100)	10.8	22.8
65	21	45	←	66	20	46	765 791.210(10)	−20.7	−8.8
90	11	79	←	90	10	80	766 833.091(50)	9.0	−30.2
92	9	83	←	92	8	84	767 466.649(120)	−62.7	−75.7
62	3	59	←	63	2	62	774 876.880(40)	29.2	28.4
71	5	67	←	72	2	70	780 862.523(30)	−9.6	−18.3
64	21	43	←	65	20	46	784 626.891(10)	8.4	18.7

Please cite this article as: Ulenikov ON, et al. Re-analysis of the (100), (001), and (020) rotational structure of SO_2 on the basis of high resolution FTIR spectra. J Quant Spectrosc Radiat Transfer (2013), http://dx.doi.org/10.1016/j.jqsrt.2013.04.011

Table 1 (*continued*)

Transition							Frequency, exp.[a] in MHz	Δ (calc)[b] in kHz	Δ (calc)[c] in kHz
1							2	3	4
63	4	60	←	64	1	63	793 524.340(20)	5.5	4.2
72	4	68	←	73	3	71	798 621.881(40)	−18.2	−29.9
73	23	51	←	74	22	52	798 697.330(150)	56.8	106.5
68	22	46	←	69	21	49	801 319.331(30)	7.8	14.8
63	21	43	←	64	20	44	803 461.207(15)	−15.5	−7.6
20	20	0	←	20	19	1	1 927 842.304(30)	−4.5	4.6
21	20	2	←	21	19	3	1 927 998.798(40)	−42.5	−35.9
22	20	2	←	22	19	3	1 928 161.366(30)	2.5	6.6
23	20	4	←	23	19	5	1 928 329.684(30)	7.9	9.9
24	20	4	←	24	19	5	1 928 503.566(40)	−1.1	−1.4
25	20	6	←	25	19	7	1 928 682.827(20)	9.4	6.9
26	20	6	←	26	19	7	1 928 867.227(20)	27.6	22.8
27	20	8	←	27	19	9	1 929 056.510(30)	33.2	26.5
29	20	10	←	29	19	11	1 929 448.742(20)	11.9	1.8
30	20	10	←	30	19	11	1 929 651.196(40)	4.8	−6.9
31	20	12	←	31	19	13	1 929 857.538(25)	19.5	6.3
32	20	12	←	32	19	13	1 930 067.441(30)	6.9	−7.5
33	20	14	←	33	19	15	1 930 280.606(40)	−45.8	−61.2
34	20	14	←	34	19	15	1 930 496.853(40)	−24.7	−40.9
35	20	16	←	35	19	17	1 930 715.784(30)	−25.6	−42.3
36	20	16	←	36	19	17	1 930 937.131(50)	−5.9	−23.3
37	20	18	←	37	19	19	1 931 160.518(30)	−24.8	−42.2
38	20	18	←	38	19	19	1 931 385.703(40)	2.6	−15.0
50	5	45	←	49	4	46	1 931 571.663(30)	−29.0	−40.3
39	20	20	←	39	19	21	1 931 612.305(30)	28.1	10.5
40	20	20	←	40	19	21	1 931 839.941(24)	9.9	−7.3
41	20	22	←	41	19	23	1 932 068.330(30)	15.6	−0.9
42	20	22	←	42	19	23	1 932 297.098(20)	28.0	12.2
43	20	24	←	43	19	25	1 932 525.788(50)	−46.2	−61.2
44	20	24	←	44	19	25	1 932 754.238(30)	2.0	−12.0
35	13	23	←	34	12	22	1 932 958.812(30)	−53.7	−44.0
45	20	26	←	45	19	27	1 932 981.907(20)	10.7	−2.5
46	20	26	←	46	19	27	1 933 208.376(60)	−53.7	−65.7
28	6	22	←	27	3	25	1 933 324.398(30)	−14.7	−36.8
47	20	28	←	47	19	29	1 933 433.460(20)	17.3	6.6
48	20	28	←	48	19	29	1 933 656.548(20)	13.6	4.0
49	20	30	←	49	19	31	1 933 877.304(40)	6.5	−2.1
50	20	30	←	50	19	31	1 934 095.318(50)	0.7	6.7
51	20	32	←	51	19	33	1 934 310.166(60)	−5.5	−11.9
59	9	51	←	58	8	50	1 934 550.591(40)	−22.3	7.7
43	8	36	←	43	5	39	1 934 705.394(40)	−18.9	20.9
53	20	34	←	53	19	35	1 934 728.672(30)	11.9	6.6
54	20	34	←	54	19	35	1 934 931.429(40)	13.4	8.4
30	14	16	←	29	13	17	1 935 046.840(20)	−7.9	−8.3
41	8	34	←	41	5	37	1 935 117.660(70)	37.2	79.9
55	20	36	←	55	19	37	1 935 129.290(40)	43.0	37.6
20	16	4	←	19	15	5	1 935 673.179(30)	10.9	5.2
25	15	11	←	24	14	10	1 935 870.169(20)	27.4	20.7
65	20	46	←	65	19	47	1 936 732.689(100)	−83.7	−135.4

Please cite this article as: Ulenikov ON, et al. Re-analysis of the (100), (001), and (020) rotational structure of SO_2 on the basis of high resolution FTIR spectra. J Quant Spectrosc Radiat Transfer (2013), http://dx.doi.org/10.1016/j.jqsrt.2013.04.011

39	8	32	↓	39	5	35	1 938 137.092(60)	14.8		59.5	
75	9	67	↓	74	8	66	1 939 206.049(200)	57.7		78.2	
46	11	35	↓	45	10	36	1 940 889.752(30)	−1.5		25.8	
58	9	49	↓	57	8	50	1 941 945.067(40)	25.3		51.0	
52	10	42	↓	51	9	43	1 945 728.205(40)	3.8		33.5	

[a] Values in parentheses are experimental uncertainties.
[b] The value $\Delta = \nu^{exp.} - \nu^{calc.}$, where $\nu^{exp.}$ is taken from Ref. [35], and $\nu^{calc.}$ is calculated with the parameters from column 2 of Table 2.
[c] The value $\Delta = \nu^{exp.} - \nu^{calc.}$, where $\nu^{exp.}$ is taken from Ref. [35], and $\nu^{calc.}$ is calculated with the parameters from column 3 of Table 2.

"allowed" transitions in the parallel bands are

$$\Delta J = 0, \pm 1, \quad \Delta K_a = 0, \quad \Delta K_c = \pm 1.$$

The selection rules for the "allowed" transitions in the perpendicular bands are

$$\Delta J = 0, \pm 1, \quad \Delta K_a = \pm 1, \quad \Delta K_c = \pm 1.$$

Besides "allowed" transitions, weak "forbidden" ones are allowed both in the parallel and perpendicular bands. The selection rules have the following form:

$$\Delta J = 0, \pm 1, \quad \Delta K_a = even, \quad \Delta K_c = odd,$$

and

$$\Delta J = 0, \pm 1, \quad \Delta K_a = odd, \quad \Delta K_c = odd.$$

In accordance with the symmetry properties, the effective Hamiltonian of the XY_2-type molecule of the C_{2v} symmetry has been discussed in the spectroscopic literature many times (see, e.g., Refs. [45–47]). For consistency, we will briefly present it here without detailed

Table 2
Spectroscopic parameters of the ground vibrational state of the SO_2 molecule (in cm^{-1}).[a]

Parameter 1	PS[b] 2	Ref. [35][c] 3
E		
A	2.02735420407(163)	2.02735433
B	0.344173882136(410)	0.3441739084
C	0.293526503766(428)	0.293526529
$\Delta_K \times 10^4$	0.864015421(289)	0.8640369
$\Delta_{JK} \times 10^5$	−0.390123832(126)	−0.3901187
$\Delta_J \times 10^6$	0.220539487(159)	0.220549
$\delta_K \times 10^6$	0.846291509(854)	0.846284
$\delta_J \times 10^7$	0.567423257(229)	0.5674232
$H_K \times 10^7$	0.12360428(155)	0.12375
$H_{KJ} \times 10^9$	−0.64960685(842)	−0.64936
$H_{JK} \times 10^{11}$	0.1160311(386)	0.116
$H_J \times 10^{12}$	0.3746170(246)	0.37589
$h_K \times 10^9$	0.5679872(101)	0.5670
$h_{JK} \times 10^{12}$	−0.243030(283)	−0.23
$h_J \times 10^{12}$	0.18300674(481)	0.1829
$L_K \times 10^{11}$	−0.2608919(349)	−0.265
$L_{KKJ} \times 10^{12}$	0.1807804(411)	0.180
$L_{JK} \times 10^{13}$	−0.1097261(451)	−0.109
$L_{JJK} \times 10^{17}$	−0.99508(476)	−0.88
$L_J \times 10^{17}$	−0.110360(128)	−0.116
$l_K \times 10^{12}$	−0.319192(117)	−0.32
$l_{KJ} \times 10^{14}$	0.254416(212)	0.27
$l_{JK} \times 10^{17}$		−0.2
$l_J \times 10^{18}$	−0.607568(294)	−0.597
$P_K \times 10^{15}$	0.584163(354)	0.649
$P_{KKJ} \times 10^{16}$	−0.408713(675)	−0.394
$P_{KJ} \times 10^{18}$	−0.623763(944)	−0.703
$P_{JK} \times 10^{19}$	0.649369(650)	0.778
$S_K \times 10^{18}$	−0.088587(130)	−0.12
$S_{KKJ} \times 10^{20}$	0.81536(427)	0.70

[a] Values in parentheses are 1σ confidence intervals (in last digits).
[b] Obtained from the fit in the present study.
[c] Recalculated from Table 3 of Ref. [35]. Number of kept digits in the values of parameters corresponds to the number of digits in the initial values from Ref. [35].

Please cite this article as: Ulenikov ON, et al. Re-analysis of the (100), (001), and (020) rotational structure of SO_2 on the basis of high resolution FTIR spectra. J Quant Spectrosc Radiat Transfer (2013), http://dx.doi.org/10.1016/j.jqsrt.2013.04.011

explanations:

$$H^{\nu,-r.}=\sum_{\nu,\tilde{\nu}}|\nu\rangle\langle\tilde{\nu}|H_{\nu\tilde{\nu}}, \quad (1)$$

where the summation extends over all (in our case, three) interacting vibrational states: $|1\rangle\equiv(100,A_1)$, $|2\rangle\equiv(020,A_1)$, and $|3\rangle\equiv(001,B_1)$. The diagonal operators $H_{\nu\nu}$ describe unperturbed rotational structures of the corresponding vibrational states. The nondiagonal operators $H_{\nu\tilde{\nu}}$, $(\nu\neq\tilde{\nu})$ describe resonance interactions (Fermi, or Coriolis) between the states $|\nu\rangle$ and $|\tilde{\nu}\rangle$. The diagonal block operators have the same form for all the three vibrational states involved (Watson's Hamiltonian in the A-reduction and I^r representation):

$$\begin{aligned}H_{\nu\nu}=&E^{\nu}+[A^{\nu}-\tfrac{1}{2}(B^{\nu}+C^{\nu})]J_z^2+\tfrac{1}{2}(B^{\nu}+C^{\nu})J^2+\tfrac{1}{2}(B^{\nu}-C^{\nu})J_{xy}^2\\&-\Delta_K^{\nu}J_z^4-\Delta_{JK}^{\nu}J_z^2J^2-\Delta_J^{\nu}J^4-\delta_K^{\nu}[J_z^2,J_{xy}^2]-2\delta_J^{\nu}J^2J_{xy}^2\\&+H_K^{\nu}J_z^6+H_{KJ}^{\nu}J_z^4J^2+H_{JK}^{\nu}J_z^2J^4+H_J^{\nu}J^6\\&+[J_{xy}^2,h_K^{\nu}J_z^4+h_{JK}^{\nu}J^2J_z^2+h_J^{\nu}J^4]\\&+L_K^{\nu}J_z^8+L_{KKJ}^{\nu}J_z^6J^2+L_{JK}^{\nu}J_z^4J^4+L_{KJJ}^{\nu}J_z^2J^6+L_J^{\nu}J^8\\&+[J_{xy}^2,l_K^{\nu}J_z^6+l_{KJ}^{\nu}J^2J_z^4+l_{JKJ}^{\nu}J^4J_z^2+l_J^{\nu}J^6]\\&+\cdots+P_K^{\nu}J_z^{10}+P_{KKKJ}^{\nu}J_z^8J^2+P_{KKJJ}^{\nu}J_z^6J^4+P_{JJK}^{\nu}J_z^4J^6\\&+S_K^{\nu}J_z^{12}+S_{KKKKJ}^{\nu}J_z^{10}J^2+\cdots\end{aligned} \quad (2)$$

where J_α $(\alpha=x,y,z)$ are the components of the angular momentum operator defined in the molecule-fixed coordinate system; $J_{xy}^2=J_x^2-J_y^2$; A^{ν}, B^{ν}, and C^{ν} are the effective rotational constants connected with the vibrational states ν, and the other parameters are the different order centrifugal distortion coefficients.

We may distinguish between two types of coupling operators $H^{\nu\tilde{\nu}}$, $(\nu\neq\tilde{\nu})$, corresponding to the two different types of resonance interactions which can occur in XY_2 (C_{2v}) asymmetric top molecules. If the product $\Gamma=\Gamma^{\nu}\otimes\Gamma^{\tilde{\nu}}$ of the symmetry species of the states ν and $\tilde{\nu}$ is equal to A_1 (*i.e.*, $\Gamma^{\nu}=\Gamma^{\tilde{\nu}}$), then the states ν and $\tilde{\nu}$ are connected by an anharmonic Fermi resonance interaction, and the corresponding interaction operator has the form

$$\begin{aligned}H_{\nu\tilde{\nu}}=&{}^{\nu\tilde{\nu}}F_0+{}^{\nu\tilde{\nu}}F_KJ_z^2+{}^{\nu\tilde{\nu}}F_JJ^2+{}^{\nu\tilde{\nu}}F_{KK}J_z^4+{}^{\nu\tilde{\nu}}F_{KJ}J_z^2J^2\\&+{}^{\nu\tilde{\nu}}F_{JJ}J^4+\cdots+{}^{\nu\tilde{\nu}}F_{xy}(J_x^2-J_y^2)+{}^{\nu\tilde{\nu}}F_{Kxy}\{J_z^2,(J_x^2-J_y^2)\}_+\\&+2{}^{\nu\tilde{\nu}}F_{Jxy}J^2(J_x^2-J_y^2)+\cdots\end{aligned} \quad (3)$$

If the product is $\Gamma=B_1$, then the states ν and $\tilde{\nu}$ are connected by a Coriolis resonance interaction of the form

$$\begin{aligned}H_{\nu\tilde{\nu}}=&iJ_yH_{\nu\tilde{\nu}}^{(1)}+H_{\nu\tilde{\nu}}^{(1)}iJ_y+\{J_x,J_z\}_+H_{\nu\tilde{\nu}}^{(2)}+H_{\nu\tilde{\nu}}^{(2)}\{J_x,J_z\}_+\\&+\{iJ_y,(J_x^2-J_y^2)\}_+H_{\nu\tilde{\nu}}^{(3)}+H_{\nu\tilde{\nu}}^{(3)}\{iJ_y,(J_x^2-J_y^2)\}_++\cdots\end{aligned} \quad (4)$$

The operators $H_{\nu\tilde{\nu}}^{(i)}$, $i=1,2,3,\ldots$ in Eq. (4) have the form

$$\begin{aligned}H_{\nu\tilde{\nu}}^{(i)}=&\tfrac{1}{2}{}^{\nu\tilde{\nu}}C^i+{}^{\nu\tilde{\nu}}C_K^iJ_z^2+\tfrac{1}{2}{}^{\nu\tilde{\nu}}C_J^iJ^2+{}^{\nu\tilde{\nu}}C_{KK}^iJ_z^4+{}^{\nu\tilde{\nu}}C_{KJ}^iJ_z^2J^2\\&+\tfrac{1}{2}{}^{\nu\tilde{\nu}}C_{JJ}^iJ^4+{}^{\nu\tilde{\nu}}C_{KKK}^iJ_z^6+{}^{\nu\tilde{\nu}}C_{KKJ}^iJ_z^4J^2\\&+{}^{\nu\tilde{\nu}}C_{KJJ}^iJ_z^2J^4+\tfrac{1}{2}{}^{\nu\tilde{\nu}}C_{JJJ}^iJ^6+\cdots\end{aligned} \quad (5)$$

To prevent confusion in the label notations used, we should mention that the axis of symmetry of the XY_2 molecule in our case is not the z-axis, but the x-axis. This fact is the consequence of using the diagonal blocks (2) of the Hamiltonian (1) in the form of Watson's operator in A-reduction and I^r-representation. However, for the point group symmetry assignment of normal modes we use the

Table 3
Statistical information for the ν_1, ν_3, and $2\nu_2$ bands of SO_2 molecule.

Band	Center in cm^{-1}	J^{max}	K_a^{max}	N_l[a]	rms_l in 10^{-5} cm^{-1}	m_{l1}[b] in %	m_{l2}[b] in %	m_{l3}[b] in %	N_t[c]	rms_t in 10^{-5} cm^{-1}	m_{t1}[b] in %	m_{t2}[b] in %	m_{t3}[b] in %
1	2	3	4	5	6	7	8	9	10	11	12	13	14
Ground													
With param. from Ref. [35][d]		92	23						149	28.2[d]			
With our param.[d]		92	23						149	22.5[d]			
With param. from Ref. [35][e]		53	34						78	269.1	3.8	11.5	84.7
With our param.[e]		53	34						78	10.8	73.1	20.5	6.4
ν_1	1151.71295												
Ref. [26] ($J\leq69/K_a\leq28$)		69	28	1216	21.0		70.7	29.3					
Our ($J\leq69/K_a\leq28$)		69	28	1562	3.9	97.3	2.4	0.3	6925	12.2	80.4	9.4	10.2
Our (total)		89	37	1913	6.1	93.3	5.1	1.6	7618	12.7	78.4	10.6	11.0
ν_3	1362.06030												
Ref. [26] ($J\leq89/K_a\leq24$)		89	24	884	21.0		70.7	29.3					
Our ($J\leq89/K_a\leq24$)		89	24	1653	8.2	87.7	9.2	3.1	3695	15.0	69.9	14.3	15.8
Our (total)		109	28	1838	9.7	84.1	10.6	5.3	3952	15.6	68.3	14.7	17.0
$2\nu_2$	1035.12639												
Our		54	9	312	13.9	68.0	20.5	11.5	561	21.1	43.6	25.1	31.3

[a] N_l is the numbers of upper levels.

[b] Here $m_i=n_i/N\times100\%$ $(i=1,2,3)$; n_1, n_2, and n_3 are the numbers of levels (transitions) for which the differences $\delta=|E^{exp.}-E^{calc.}|$ (for columns 7–9), or $\delta=|\nu^{exp}-\nu^{calc}|$ (for columns 12–14) satisfy the conditions $\delta\leq10\times10^{-5}$ cm^{-1}, 10×10^{-5} $cm^{-1}<\delta\leq20\times10^{-5}$ cm^{-1}, and $\delta>20\times10^{-5}$ cm^{-1}.

[c] N_t is the numbers of transitions.

[d] Reproduction of sub-millimeter wave transitions from Ref. [35]: $K_a\leq23$. The *rms* in column 11 is in kHz.

[e] Reproduction of Ground State Combination Differences obtained from analysis of our FTIR experimental data: $29\leq K_a\leq34$.

Please cite this article as: Ulenikov ON, et al. Re-analysis of the (100), (001), and (020) rotational structure of SO_2 on the basis of high resolution FTIR spectra. J Quant Spectrosc Radiat Transfer (2013), http://dx.doi.org/10.1016/j.jqsrt.2013.04.011

standard convention with $z=C_2$. For further, more detailed discussion of this type of effective Hamiltonian model we refer to [45].

4. Analysis of spectra and re-determination of ground state spectroscopic parameters

Survey weak spectrum of the ν_1 and ν_3 bands of the SO_2 molecule is shown on the upper part of Fig. 1. Fig. 2 presents the S-spectrum of the ν_1 band. In this case, the P-branch of very weak $2\nu_2$ band is seen in the lower wavenumber region. For illustration of quality of the experimentally recorded spectra, upper part of Fig. 3 presents small portion of the high resolution spectrum in the R-branch of the ν_1 band. As the analysis showed, in both the ν_1 and ν_3, and $2\nu_2$ bands, at least, two of three (P-, Q-, and/or R-) branches are clearly pronounced. As a consequence, one can expect a good fulfillment of the "ground state combination differences" principle.

In the analysis of the recorded spectra we were able to assign transitions with the maximum values of quantum numbers $J^{max.}=109$ and $K_a^{max.}=37$. Correctness of assignments was controlled by the construction of corresponding "experimental" Ground State Combination Differences. It was found that, starting with the value of quantum number $K_a=26$–27, difference between GSCD values obtained from experimental transitions and calculated ones obtained by the best set of the ground state rotational parameters, Ref. [35], starts increasing quickly with increase of quantum number K_a. In this case, differences between "experimental" and "calculated" GSCD values were increased from about $1–1.5\times10^{-4}$ cm^{-1} for $K_a\leq25$ up to 60.5×10^{-4} cm^{-1} for $K_a=34$. This circumstance becomes clear if one takes into account that in [35] the ground state rotational parameters were obtained on the basis of high-accurate experimental sub-millimeter wave transitions with the maximum value of quantum number $K_a^{max.}=23$. For this reason, in the present paper we re-analyze the rotational structure of the SO_2 ground vibrational state on the basis of the ground state

Table 4
Spectroscopic parameters of the (100), (001), and (020) vibrational states of the SO_2 molecule (in cm^{-1}).[a]

Parameter 1	(100), our 2	(100) from [26] 3	(001), our 4	(001) from [26] 5	(020), our 6	(020) from [26] 7
E	1151.68575415 (466)	1151.712950	1362.06030242(716)	1362.060336	1035.1535902 (118)	1035.126371
A	2.0284219524 (969)	2.028436263	2.006648486 (197)	2.006644631	2.107666447 (651)	2.107649092
B	0.3425072831 (280)	0.3425122666	0.3430035682 (288)	0.3430079384	0.3443180685 (580)	0.3443172408
C	0.2922516577 (118)	0.2921140821	0.2922918154 (122)	0.2924294870	0.2924639658 (337)	0.2924635974
$\Delta_K\times10^4$	0.87785264 (873)	0.87644839	0.8487019 (198)	0.8503404	1.0631021 (904)	1.0638447
$\Delta_{JK}\times10^5$	−0.3905198 (726)	−0.37655179	−0.3921223 (802)	−0.4069928	−0.4255028 (501)	−0.4257225
$\Delta_J\times10^6$	0.2193355 (109)	0.21977784	0.2234330 (110)	0.22308590	0.2216133 (260)	0.2212268
$\delta_K\times10^6$	0.846291509	0.922469	0.8542019 (820)	0.7891669	1.23853 (158)	1.236181
$\delta_J\times10^7$	0.5676407 (604)	0.5653892	0.5719439 (545)	0.5743462	0.574481 (140)	0.5742303
$H_K\times10^7$	0.1272614 (117)	0.1283702	0.1202984 (677)	0.120473	0.182918	0.188955
$H_{KJ}\times10^9$	−0.656738 (253)	−0.715856	−0.651555 (295)	−0.608500	−0.8644971	−0.86163
$H_{JK}\times10^{11}$	0.1160311	0.1325	0.1160311	0.94826	0.79840	0.554
$H_J\times10^{12}$	0.371073 (328)	0.38265	0.383059 (564)	0.37734	0.373265	0.26162
$h_K\times10^9$	0.5679872	0.553916	0.577289 (542)	0.90549	0.954963	0.927
$h_{JK}\times10^{12}$	−0.243030	−0.37865	−0.243030	−0.37865	−1.3097	−2.78
$h_J\times10^{12}$	0.184502 (319)	0.178527	0.184898 (178)	0.190584	0.183500	0.194
$L_K\times10^{11}$	−0.271360 (112)	−0.280590	−0.24940 (108)	−0.26921	−0.478860	−0.437
$L_{KKJ}\times10^{12}$	0.1868310(860)	0.125454	0.175030 (216)	0.16636	0.29657	0.158
$L_{JK}\times10^{13}$	−0.110391 (183)	0.007728	−0.1097261	0.007728	−0.1993	
$L_{JJK}\times10^{16}$	−0.099508	−1.2014	−0.099508	−1.8914	−0.7190	
$L_J\times10^{17}$	−0.110360	−0.3099	−0.10166 (312)	−0.2910	−0.0957	
$l_K\times10^{12}$	−0.324991 (886)		−0.315084(552)		−0.5895	
$l_{KJ}\times10^{14}$	0.284853 (540)		0.254416		0.273	
$l_{JK}\times10^{17}$					−0.24	
$l_J\times10^{18}$	−0.607568		−0.607568		−0.69185	
$P_K\times10^{15}$	0.599887 (390)	0.68478	0.55386 (604)	0.7101	1.443	
$P_{KKJ}\times10^{16}$	−0.408713	−0.26122	−0.408713	−0.26122	−0.78360	
$P_{KJ}\times10^{18}$	−0.623763		−0.623763		−1.286	
$P_{JK}\times10^{19}$	0.649369		0.649369		1.666	
$S_K\times10^{19}$	−0.88587		−0.88587		−3.30	
$S_{KKJ}\times10^{20}$	0.81536		0.81536		1.615	

[a] Values in parentheses are 1σ standard errors. Parameters presented without standard errors have been fixed to the values of the ground vibrational state ((100) and (001) states) from column 2 of Table 2, or to the values ((020) state) estimated in accordance with the formula (6).

Please cite this article as: Ulenikov ON, et al. Re-analysis of the (100), (001), and (020) rotational structure of SO_2 on the basis of high resolution FTIR spectra. J Quant Spectrosc Radiat Transfer (2013), http://dx.doi.org/10.1016/j.jqsrt.2013.04.011

combination differences determined in the frame of analysis of our FTIR experimental data (in this case, 78 FTIR combination differences with the values $J^{max.}=53$ and $K_a^{max.}=34$ were used). The 149 sub-millimeter wave transitions from Ref. [35] (they are reproduced in column 2 of Table 1) were also added to the set of initial data used in the fit of the ground state spectroscopic parameters. The values of parameters obtained from the weighted fit are presented in column 2 of Table 2. Values in parenthesis are 1σ statistical confidence intervals. For comparison, column 3 of Table 2 presents the values of the ground state spectroscopic parameters that are reproduced from Ref. [35]. One can see good correlation between both sets of parameters. At the same time our new set of parameters not only reproduce better the FTIR Ground State Combination Differences (the *rms* deviation of 78 GSCD, $29\geq K_a\geq 34$, obtained from our experimental data, being calculated with the parameters from Ref. [35] is 269.1×10^{-5} cm^{-1}; being calculated with our set of parameters, that value is decreased up to 10.8×10^{-5} cm^{-1}, see statistical Table 3 for more details), but also reproduces with the better rms-deviation values the sub-millimeter wave line positions from Ref. [35] (compare columns 3 and 4 of Table 1; the *rms* deviation is 28.2 kHz and 22.5 kHz at calculation with parameters from [35] and our parameters from column 2 of Table 2, respectively). The number of fitted parameters in our case is even less than in [35].

Table 5
Resonance interaction parameters for the (100), (020), and (001) vibrational states of the SO_2 molecule (in cm^{-1}).[a]

Parameter	Value
${}^{(100),(020)}F_0$	1.78
${}^{(100),(001)}C^1$	−0.17
${}^{(100),(001)}C^3\times10^6$	0.31773(644)
${}^{((100),(020)}F_{Kxy}\times10^7$	0.714042(816)
${}^{(100),(001)}C_K^1\times10^4$	−0.16849(214)
${}^{(100),(001)}C_J^3\times10^{11}$	−0.2335(125)
${}^{(100),(001)}C^2\times10^2$	0.20827(167)

[a] Values in parentheses are 1σ standard errors. Parameters presented without standard errors have been estimated on the basis of the potential energy surface parameters of SO_2 from Ref. [48] and were constrained in the fit.

5. Re-analysis of the rotational structures of the vibrational states (100), (001), and (020)

The new ground state parameters obtained in Section 4 were used then for calculation of ground state rotational energies which, in turn, were used in the re-assignments of transitions in the recorded FTIR spectra. The list of more than 12 130 finally assigned transitions is presented in the Supplementary Materials (see also the statistical information in Table 3). From these transitions we obtained 4063 upper ro-vibrational energies (1913, 1838, and 312 upper energies for the states (100), (001), and (020), respectively) which were used then as input data in a weighted least square fit with the aim to determine rotational, centrifugal distortion, and resonance interaction parameters of the

Table 6
Heterodyne frequencies of SO_2 in the ν_3 band.

Transition 1	Frequency, exp.[a] in MHz 2	ΔI,[b] in MHz 3	ΔII,[c] in MHz 4	Transition 1	Frequency, exp.[a] in MHz 2	ΔI,[b] in MHz 3	ΔII,[c] in MHz 4
${}^qP_6(18)$	40 457 019.8(5.0)	1.5	−0.3	${}^qR_1(13)$	41 079 955.2(5.0)	1.5	0.3
${}^qP_0(20)$	40 458 986.4(5.0)	1.4	0.0	${}^qR_5(13)$	41 080 193.8(3.0)	−3.1	−4.6
${}^qP_{10}(16)$	40 460 775.5(9.0)	3.5	2.0	${}^qR_{10}(26)$	41 267 578.4(5.0)	−1.0	−1.9
${}^qP_8(17)$	40 461 362.9(5.0)	0.3	−1.2	${}^qR_6(24)$	41 271 076.8(4.0)	0.6	−0.9
${}^qP_2(19)$	40 462 193.6(5.0)	2.1	0.6	${}^qR_8(25)$	41 271 318.4(4.0)	−0.7	−1.9
${}^qP_5(18)$	40 463 046.5(5.0)	2.1	0.6	${}^qR_{11}(27)$	41 272 779.1(4.0)	−1.4	−1.7
${}^qP_2(18)$	40 464 934.6(5.0)	1.5	0.3	${}^qR_1(25)$	41 275 291.4(4.0)	1.3	−0.2
${}^qQ_{12}(21)$	40 734 536.6(4.0)	0.4	−0.5	${}^qR_8(38)$	41 494 155.7(6.0)	1.2	0.6
${}^qP_2(5)$	40 734 999.1(4.0)	−0.8	−1.7	${}^qR_{12}(41)$	41 495 464.1(8.0)	−0.8	−0.5
${}^qQ_{12}(20)$	40 735 926.4(4.0)	−0.5	−1.7	${}^qR_6(37)$	41 496 666.6(4.0)	1.0	−0.2
${}^qQ_{12}(19)$	40 737 249.7(4.0)	−1.7	−2.9	${}^qR_4(37)$	41 499 389.5(4.0)	0.0	−1.8
${}^qQ_{12}(18)$	40 738 508.3(4.0)	−1.3	−2.5	${}^qR_3(36)$	41 500 253.4(4.0)	1.1	−0.7
${}^qP_1(5)$	40 740 637.5(4.0)	1.8	0.9	${}^qR_5(37)$	41 502 232.2(4.0)	1.0	−0.5
${}^qQ_{12}(16)$	40 740 829.0(4.0)	1.4	0.2	${}^qR_0(40)$	41 504 180.9(6.0)	2.2	1.6
${}^qQ_{11}(25)$	40 741 496.8(4.0)	1.3	0.7	${}^qR_7(38)$	41 504 742.1(5.0)	0.1	−0.8
${}^qQ_{12}(15)$	40 741 887.7(4.0)	0.6	−0.9	${}^qR_{10}(40)$	41 504 915.0(6.0)	−1.1	−1.1
${}^qQ_{12}(13)$	40 743 809.8(6.0)	2.3	0.8	${}^qR_2(38)$	41 505 369.2(4.0)	1.3	−0.8
${}^qR_0(2)$	40 890 362.9(6.0)	13.1	12.0	${}^qR_8(56)$	41 792 579.5(4.0)	−1.0	−0.1
${}^qR_3(7)$	40 979 127.8(20.0)	5.7	4.5	${}^qR_{10}(58)$	41 793 377.8(5.0)	−1.9	−5.8
${}^qR_6(8)$	40 981 712.6(10.0)	−1.0	−2.4	${}^qR_{11}(59)$	41 794 759.0(4.0)	−2.5	−1.6
${}^qR_8(9)$	40 983 895.9(9.0)	2.6	1.1	${}^qR_3(58)$	41 796 023.8(6.0)	−3.7	−3.7
${}^qR_5(8)$	40 988 165.8(15.0)	−4.4	−5.9	${}^qR_1(60)$	41 796 222.6(5.0)	0.5	2.9
${}^qR_8(14)$	41 075 376.3(3.0)	1.3	−0.2	${}^qR_5(57)$	41 796 860.0(5.0)	0.0	−0.6
${}^qR_{11}(16)$	41 078 597.4(6.0)	2.6	1.1				

[a] Values in parentheses are experimental uncertainties (in MHz).
[b] The value $\Delta I=\nu^{exp.}-\nu^{calc.}$, where $\nu^{exp.}$ is taken from Ref. [23], and $\nu^{calc.}$ is calculated with the parameters from column 2 of Table 2, columns 2, 4, 6 of Table 4 and 5.
[c] The values $\Delta II=\nu^{exp.}-\nu^{calc.}$ are reproduced from the last column of Table V, Ref. [26].

Please cite this article as: Ulenikov ON, et al. Re-analysis of the (100), (001), and (020) rotational structure of SO_2 on the basis of high resolution FTIR spectra. J Quant Spectrosc Radiat Transfer (2013), http://dx.doi.org/10.1016/j.jqsrt.2013.04.011

Table 7
Heterodyne frequencies of SO_2 in the ν_1 band.

Transition 1	Wavenumber, exp.[a] in cm^{-1} 2	ΔI[b] 3	ΔII[c] 4	Transition 1	Wavenumber, exp.[a] in cm^{-1} 2	ΔI[b] 3	ΔII[c] 4
$^pP_{10}(48)$	1085.8791(2)	3.0	2.5	$^pP_{13}(43)$	1079.6768(2)	0.7	0.3
$^pP_{13}(35)$	1085.7302(2)	−0.6	−0.8	$^pP_{17}(26)$	1079.6722(2)	0.9	0.0
$^pP_{16}(22)$	1085.6640(2)	−0.4	−1.2	$^pP_{18}(23)$	1078.7424(2)	−1.6	−2.7
$^pP_{11}(45)$	1084.7518(2)	1.5	1.2	$^pP_{14}(40)$	1078.7327(2)	−3.4	−3.8
$^pP_{14}(32)$	1084.7412(2)	1.0	0.7	$^pP_{15}(36)$	1078.5654(2)	−0.9	−1.4
$^pP_{17}(19)$	1084.6661(2)	0.2	−0.9	$^pP_{19}(19)$	1078.5249(2)	1.5	0.2
$^pP_{15}(28)$	1084.4941(2)	0.6	0.1	$^pP_{16}(32)$	1078.3954(2)	0.3	−0.3
$^pP_{10}(51)$	1083.6276(2)	0.9	0.3	$^pP_{17}(29)$	1077.4839(2)	2.4	1.6
$^pQ_{21}(31)$	1083.5631(2)	0.3	1.5	$^pP_{13}(46)$	1077.3667(2)	0.7	0.1
$^pP_{16}(25)$	1083.5164(2)	−0.8	−1.5	$^pP_{25}(18)$	1077.3043(2)	0.2	−0.8
$^pP_{13}(38)$	1083.4793(2)	0.5	0.2	$^pP_{12}(52)$	1076.0146(2)	−1.7	−2.6
$^pQ_{21}(32)$	1083.4529(2)	1.5	2.8	$^pP_{17}(31)$	1076.0089(2)	−0.1	−0.9
$^pP_{9}(56)$	1083.4368(2)	0.1	−0.4	$^pP_{18}(27)$	1075.8530(2)	−0.2	−1.1
$^pQ_{21}(33)$	1083.3391(2)	0.2	1.6	$^pP_{20}(20)$	1074.7958(2)	1.1	0.2
$^pP_{14}(34)$	1083.2556(2)	−3.0	−3.3	$^pP_{15}(41)$	1074.7655(2)	−1.1	−1.8
$^pP_{17}(22)$	1082.5452(2)	−0.6	−1.6	$^pP_{16}(37)$	1074.6457(2)	0.4	−0.3
$^pP_{14}(35)$	1082.5091(2)	0.9	0.5	$^pP_{17}(33)$	1074.5217(2)	0.1	−0.6
$^pP_{11}(48)$	1082.4653(2)	−1.0	−1.6	$^pP_{19}(28)$	1072.0598(2)	−0.3	−1.2
$^pP_{15}(31)$	1082.2932(2)	−0.5	−1.0	$^pP_{20}(24)$	1071.9389(2)	1.0	0.3
$^pP_{18}(18)$	1082.2808(2)	−1.0	−2.3	$^pP_{14}(49)$	1071.7722(2)	−2.0	−2.8
$^pP_{12}(44)$	1082.1895(2)	0.1	−0.3	$^pP_{18}(34)$	1070.6730(2)	1.0	0.2
$^pP_{16}(27)$	1082.0690(2)	0.9	0.3	$^pP_{20}(26)$	1070.4904(2)	−0.1	−0.6
$^pP_{16}(28)$	1081.3403(2)	−1.0	−1.7	$^pP_{22}(21)$	1070.3808(2)	−0.1	0.3
$^pP_{17}(24)$	1081.1152(2)	0.7	−0.2	$^pP_{18}(36)$	1069.1647(2)	1.3	0.5
$^pP_{14}(37)$	1081.0069(2)	0.5	0.2	$^pP_{19}(32)$	1069.1017(2)	−0.3	−1.0
$^pP_{18}(20)$	1080.8756(2)	1.5	0.2	$^pP_{20}(28)$	1069.0289(2)	0.9	0.5
$^pP_{12}(47)$	1079.8872(2)	−0.2	−0.4	$^pP_{21}(24)$	1068.9440(2)	0.6	1.1
$^pP_{16}(30)$	1079.8739(2)	−1.6	−2.2				

[a] Values in parentheses in column 2 are experimental uncertainties (in 10^{-4} cm^{-1}).
[b] The value $\Delta I = \nu^{exp.} - \nu^{calc.}$ (in 10^{-4} cm^{-1}), where $\nu^{exp.}$ is taken from Refs. [12,26], and $\nu^{calc.}$ is calculated with the parameters from column 2 of Table 2, columns 2, 4, 6 of Tables 4 and 5.
[c] The values $\Delta II = \nu^{exp.} - \nu^{calc.}$ (in 10^{-4} cm^{-1}) are reproduced from the before last column of Table VI, Ref. [26].

states (100), (001), and (020). Numerous resonance interactions between all three vibrational states were taken into account.

The fit was made with the Hamiltonian model discussed in Section 3. The initial values of rotational and centrifugal distortion parameters of the (100) and (001) states were taken to be equal to the values of corresponding parameters of the ground vibrational state. The initial values of spectroscopic parameters of the (020) state were estimated in accordance with the formula

$$P^{(020)} = P^{(000)} + 2(P^{(010)} - P^{(000)}), \quad (6)$$

where $P^{(000)}$ or $P^{(010)}$ is any of rotational or centrifugal distortion parameter of the ground or (010) vibrational state from Ref. [35], respectively; $P^{(020)}$ is a corresponding estimated parameter of the (020) vibrational state. The values of two main resonance interaction parameters, $^{(100),(020)}F_0$ and $^{(100),(001)}C^1$, have been estimated on the basis of the potential energy surface parameters of SO_2 from Ref. [48] and were constrained in the fit. The reason for the last was in the following. It is known (see, e.g., Refs. [49,50]) that the main both Fermi- and Coriolis-interaction parameters are strongly correlated with pure vibrational energies, E^v, or effective rotational parameters, A^v, B^v, C^v, respectively. In our case, when we tried to vary the $^{(100),(020)}F_0$ and/or $^{(100),(001)}C^1$ parameters, their absolute values change more than twice that is absolutely unsuitable from the physical point of view. For this reason we preferred to fix values of these parameters to theoretically estimated ones.

Results of the fit with the Hamiltonian, Eqs. (1)–(5), are presented in columns 2, 4, and 6 of Table 4 and in Table 5 (values in parentheses are 1σ statistical confidence intervals). Parameters presented without confidence intervals have been constrained to their initial values (see above). To take into account numerous accidental resonance interactions between all three studied vibrational states, (100), (001), and (020) (especially for high values of quantum numbers J and K_a), we introduced into consideration some resonance interaction parameters. They are presented in Table 5 together with their 1σ confidence intervals (in parentheses). In this case, values of the main resonance interaction parameters, $^{(100),(020)}F_0$ and $^{(100),(001)}C^1$, were constrained to their predicted ones (see above). To compare results of the present study with the previous ones, columns 3, 5, and 7 of Table 4 show the values of spectroscopic parameters from earlier study, Ref. [26]. One can see good correlation between both sets of parameters. At the same time our parameters reproduce better our FTIR experimental data. In particular, the 4063 ro-vibrational energies obtained from our experimental data are reproduced by our set of parameters with the $d_{rms} = 8.7 \times 10^{-5}$ cm^{-1}. For comparison, the same 4063 ro-vibrational energies are reproduced by the parameters from Ref. [26] with the $d_{rms} = 3329.5 \times 10^{-5}$ cm^{-1} (see

Please cite this article as: Ulenikov ON, et al. Re-analysis of the (100), (001), and (020) rotational structure of SO_2 on the basis of high resolution FTIR spectra. J Quant Spectrosc Radiat Transfer (2013), http://dx.doi.org/10.1016/j.jqsrt.2013.04.011

Table 8
MW frequencies of SO_2 in the ν_1 band.

Transition 1							Frequency, exp. in MHZ 2	Δ,[a] in MHZ 3
1	1	1	←	0	0	0	69 566.06	0.09
1	1	1	←	2	0	2	12 522.89	0.17
2	1	1	←	2	0	2	53 595.80	0.10
3	2	2	←	4	1	3	70 293.43	0.04
4	1	3	←	4	0	4	59 260.96	−0.21
4	2	2	←	5	1	5	70 765.92	0.09
5	2	4	←	6	1	5	24 275.46	0.10
6	1	5	←	6	0	6	68 951.16	−0.69
6	2	4	←	7	1	7	44 794.50	0.02
8	1	7	←	7	2	6	24 301.59	0.35
8	2	6	←	9	1	9	24 888.00	0.04
10	2	8	←	11	1	11	12 597.69	0.14
10	3	7	←	11	2	10	53 378.90	−0.29
12	2	10	←	13	1	13	9172.50	0.26
12	3	9	←	13	2	12	21 768.64	0.20
14	2	12	←	13	3	11	45 911.10	−0.11
14	2	12	←	15	1	15	15 230.50	0.14
15	4	12	←	16	3	13	40 720.80	−0.07
16	2	14	←	17	1	17	30 700.50	−0.05
17	2	16	←	16	3	13	27 386.15	−0.07
16	4	12	←	17	3	15	33 996.10	0.05
19	2	18	←	18	3	15	41 642.40	0.03
21	2	20	←	20	3	17	46 929.50	0.38
21	3	19	←	20	4	16	35 084.30	−0.02
21	5	17	←	22	4	18	26 977.80	−0.04
22	5	17	←	23	4	20	14 974.30	0.03
24	4	20	←	23	5	19	19 226.75	−0.05
25	4	22	←	24	5	19	23 788.00	0.04
26	6	20	←	27	5	23	37 515.60	−0.07
27	6	22	←	28	5	23	12 563.00	−0.04
30	5	25	←	29	6	24	32 381.80	−0.13
31	5	27	←	30	6	24	43 878.40	−0.18
31	7	25	←	32	6	26	40 163.00	0.01
32	7	25	←	33	6	28	20 835.10	−0.03
35	6	30	←	34	7	27	20 689.80	−0.02
36	8	28	←	37	7	31	45 834.00	−0.16
37	8	30	←	38	7	31	24 431.80	−0.15
40	7	33	←	39	8	32	17 994.70	0.23
41	7	35	←	40	8	32	37 593.40	0.27
42	9	33	←	43	8	36	29 668.00	−0.12
46	8	38	←	45	9	37	33 733.40	0.09

[a] The value $\Delta = \nu^{exp.} - \nu^{calc.}$, where $\nu^{exp.}$ is taken from Ref. [26], and $\nu^{calc.}$ is calculated with the parameters from column 2 of Table 2, columns 2, 4, 6 of Tables 4 and 5.

also statistical information in Table 3). In this case, differences between experimental energy values and ones calculated with the parameters from Ref. [26] are increased quickly with the increase of K_a quantum number, and for K_a=37 the difference reaches the value of 0.62 cm^{-1}.

As one more illustration of the correctness of our results, we send the reader to Tables 6–8. Columns 2 of these tables reproduce high accurate heterodyne experimental line positions of the ν_3 band from Ref. [23] (Table 6), ν_1 band from Ref. [12] (Table 7), and microwave rotational transitions in the excited (100) vibrational state (Table 8) from Ref. [26], respectively. Columns 3 of these three tables present the values of differences Δ between experimental line positions and corresponding values calculated with our parameters. One can see that values of Δ are not worse than the experimental uncertainties (the lasts are given in parentheses in column 2 of Tables 6 and 7). Columns 4 of Tables 6 and 7 present, for comparison, corresponding Δ−values from Ref. [26]. It is important to note that the experimental data from columns 2 of Tables 6–8 were not used in our fit as an input data. It means that one can consider results shown in the columns 3 of Tables 6–8, as a prediction. At the same time, our predicted Δ−values are, at least, not worse than ones from Ref. [26] (compare columns 3 and 4 of Tables 6 and 7) in spite of the fact that both the heterodyne and MW data reproduced in column 2 of Tables 6–8 were used in the fit of Ref. [26].

6. Conclusion

We re-analyzed the high resolution ro-vibrational structures of the ν_1 and ν_3 vibrational bands and, as a result, assigned about two times more transitions than was made before. Moreover, the weak $2\nu_2$ band has been observed and analyzed for the first time. We determined parameters of the Hamiltonian that reproduce the initial "experimental" ro-vibrational energies of the states (100), (001), and (020) with the *rms* deviation of 6.1×10^{-5} cm^{-1}, 9.7×10^{-5} cm^{-1}, and 13.9×10^{-5} cm^{-1}, respectively, that is close to uncertainties in experimental line positions.

Acknowledgments

The work was partially supported under the project 2.3684.2011 of Tomsk State University and FTP, Contracts 14.B37.21.0911 and 14.B37.21.1298.

Appendix A. Supplementary data

Supplementary data associated with this article can be found in the online version at http://dx.doi.org.10.1016/j.jqsrt.2013.04.011.

References

[1] Hinkley ED, Calawa AR, Kelley PJ, Clough SA. Tunable-laser spectroscopy of the ν_1 band of SO_2. J Appl Phys 1972;43:3222–4.
[2] Tejwani GD. Calculation of pressure-broadened linewidths of the SO_2 and NO_2. J Chem Phys 1972;57:4676–82.
[3] Yang WH, Roberts JA, Tejwani GD. Linewidth parameters for $\Delta J = 1, 0 \leq J \leq 43$, rotational transitions of the sulfur dioxide molecule. J Chem Phys 1973;58:4916–8.
[4] Barbe A, Secroun C, Jouve P, Duterage B, Monnanteuil N, Bellet J, et al. High resolution spectra of $\nu_1 + \nu_3$ and $(\nu_1 + \nu_2 + \nu_3) - \nu_2$ bands of SO_2. J Mol Spectrosc 1975;55:319–50.
[5] Steenbeckeliers G, Bellet J. New interpretation of the far-infrared SO_2 laser spectrum. J Appl Phys 1975;46:2620–6.
[6] Pilon PJ, Young C. Absolute integrated intensity for the ν_1 sulfur dioxide band. J Quant Spectrosc Radiat Transfer 1976;16:1137–40.
[7] Barbe A, Secroun C, Jouve P, Duterage B, Monnanteuil N, Bellet J. Spectre infrarouge haute résolution de la bande ν_1, ν_3 de la molécule $^{34}S^{16}O_2$. Mol Phys 1977;34:127–30.
[8] Pine AS, Moulton PF. Doppler-limited and atmospheric spectra of the 4−μm $\nu_1 + \nu_3$ combination band of SO_2. J Mol Spectrosc 1977;64:15–30.
[9] Pine AS, Dresselhaus G, Palm B, Davies RW, Clough SA. Analysis of the 4−μm $\nu_1 + \nu_3$ combination band of SO_2. J Mol Spectrosc 1977;67:386–415.
[10] Moskalenko NI, Terzi VF, Parzhin SN, Pushkin VT, Sadydov RS. Investigation of sulfur dioxide absorption spectra in the infrared. Izv Acad Sci USSR Atmos Oceanic Phys 1978;14:901–2.

Please cite this article as: Ulenikov ON, et al. Re-analysis of the (100), (001), and (020) rotational structure of SO_2 on the basis of high resolution FTIR spectra. J Quant Spectrosc Radiat Transfer (2013), http://dx.doi.org/10.1016/j.jqsrt.2013.04.011

[11] Herlemont F, Lyszyk M, Lemaire J. Infrared spectroscopy of OCS, SO_2, O_3 with a CO_2 waveguide laser. J Mol Spectrosc 1979;77:69–75.
[12] Satler JP, Worchesky TL, Lafferty WJ. Diode laser heterodyne spectroscopy on the ν_1 band of sulfur dioxide. J Mol Spectrosc 1981;88:364–71.
[13] Kunitomo T, Masuzaki H, Ueoka S, Osumi M. Experimental studies of the radiative properties of sulfur dioxide. J Quant Spectrosc Radiat Transfer 1981;25:345–9.
[14] Kim K, King WT. Integrated infrared intensities and the atomic polar tensors in SO_2. J Chem Phys 1984;80:969–73.
[15] Carlotti M, Di Lonardo G, Fusina L, Carli B, Mencaraglia F. The submillimeter-wave spectrum and spectroscopic constants of SO_2 in the ground state. J Mol Spectrosc 1984;106:235–44.
[16] Guelachvili G, Ulenikov ON, Ushakova GA. Analysis of the ν_1 and ν_3 absorption bands of $^{32}S^{16}O_2$. J Mol Spectrosc 1984;108:1–5.
[17] Guelachvili G, Naumenko OV, Ulenikov ON. Analysis of the Fourier-transform SO_2 absorption spectrum in the $\nu_2+\nu_3$ band. Appl Opt 1984;23:2862–7.
[18] Helminger PA, DeLuchia FC. The submillimeter wave spectrum of $^{32}S^{16}O_2$, $^{32}S^{16}O_2(\nu_2)$, and $^{34}S^{16}O_2$. J Mol Spectrosc 1985;111:66–72.
[19] J Lovas A. Microwave spectra of molecules of astrophysical interest. XXII. Sulfur dioxide (SO_2). J Phys Chem Ref Data 1985;14:395–488.
[20] Guelachvili G, Naumenko OV, Ulenikov ON. Analysis of the SO_2 absorption Fourier spectrum in regions 1055 to 2000 and 2200 to 2550 cm^{-1}. J Mol Spectrosc 1987;125:128–39.
[21] Coudert L, Maki AG, Olson WB. High-resolution measurements of the ν_2 and $2\nu_2-\nu_2$ bands of SO_2. J Mol Spectrosc 1987;124:437–42.
[22] Guelachvili G, Naumenko OV, Ulenikov ON. On the analysis of some hyperweak absorption bands of SO_2 in the regions 1055–2000 and 2200–2550 cm^{-1}. J Mol Spectrosc 1988;131:400–2.
[23] Vanek MD, Wells JS, Maki AG, Burkholder JM. Heterodyne frequency measurements on SO_2 near 41 THz (1370 cm^{-1}). J Mol Spectrosc 1990;141:346–7.
[24] Kuhnemann F, Heiner Y, Sumpf B, Hermann K. Line broadening in the ν_3 band of SO_2: studied with diode laser spectroscopy. J Mol Spectrosc 1992;152:1–12.
[25] Lafferty WJ, Fraser GT, Pine AS, Flaud J-M, Camy-Peyret C, Dana V, et al. The 3 ν_3 band of $^{32}S^{16}O_2$: line positions and intensities. J Mol Spectrosc 1992;154:51–60.
[26] Flaud JM, Perrin A, Salah LM, Lafferty WJ, Guelachvili G. A Reanalysis of the (010), (020), (100), and (001) rotational levels. J Mol Spectrosc 1993;160:272–8.
[27] Flaud JM, Lafferty WJ. $^{32}S^{16}O_2$: a refined analysis of the $3\nu_3$ band and determination of equilibrium rotational constants. J Mol Spectrosc 1993;161:396–402.
[28] Lafferty WJ, Pine AS, Flaud JM, Camy-Peyret C. The $2\nu_3$ Band of $^{32}S^{16}O_2$: line positions and intensities. J Mol Spectrosc 1993;157: 499–511.
[29] Sumpf B, Fleischmann O, Kronfeldt HD. Self-, air-, and nitrogen-broadening in the ν_1 band of SO_2. J Mol Spectrosc 1996;176:127–32.
[30] Sumpf B, Schone M, Kronfeldt HD. Self- and air-broadening in the ν_3 band of SO_2. J Mol Spectrosc 1996;179:137–41.
[31] Lafferty WJ, Pine AS, Hilpert G, Sams RL, Flaud JM. The $\nu_1+\nu_3$ and $2\nu_1+\nu_3$ band systems of SO_2: line positions and intensities. J Mol Spectrosc 1996;176:280–6.
[32] Chu PM, Wetzel SJ, Lafferty WJ, Perrin A, Flaud J-M, Arcas Ph, et al. Line intensities for the 8-μm bands of the SO_2. J Mol Spectrosc 1998;189:55–63.
[33] Lafferty WJ, Flaud JM, Guelachvili G. Analysis of the $2\nu_1$ band system of SO_2. J Mol Spectrosc 1998;188:106–7.
[34] Belov SP, Tretyakov MY, Kozin IN, Klisch E, Winnewisser G, Lafferty WJ, et al. High frequency transitions in the rotational spectrum of SO_2. J Mol Spectrosc 1998;191:17–27.
[35] Müller HSP, Brünken S. Accurate rotational spectroscopy of sulfur dioxide, SO_2, in its ground vibrational and first excited bending states, $\nu_2=0$, 1, up to 2 THz. J Mol Spectrosc 2005;232:213–22.
[36] Ulenikov ON, Bekhtereva ES, Horneman VM, Alanko S, Gromova OV. High resolution study of the $3\nu_1$ band of SO_2. J Mol Spectrosc 2009;255:111–21.
[37] Ulenikov ON, Bekhtereva ES, Horneman VM, Alanko S, Gromova OV, Leroy C. On the high resolution spectroscopy and intramolecular potential function of SO_2. J Mol Spectrosc 2009;257:137–56.
[38] Ulenikov ON, Bekhtereva ES, Gromova OV, Alanko S, Horneman VM, Leroy C. Analysis of highly excited "hot" bands in the SO_2 molecule: $\nu_2+3\nu_3-\nu_2$ and $2\nu_1+\nu_2+\nu_3-\nu_2$. Mol Phys 2010;108:1253–61.
[39] Ulenikov ON, Gromova OV, Bekhtereva ES, Bolotova IB, Leroy C, Horneman VM, et al. High resolution study of the $\nu_1+2\nu_2-\nu_2$ and $2\nu_2+\nu_3-\nu_2$ "hot" bands and ro-vibrational re-analysis of the $\nu_1+\nu_2/\nu_2+\nu_3/3\nu_2$ polyad of the $^{32}SO_2$ molecule. J Quant Spectrosc Radiat Transfer 2011;112:486–512.
[40] Ulenikov ON, Gromova OV, Bekhtereva ES, Bolotova IB, Konov IA, Horneman VM, et al. High resolution analysis of the SO_2 spectrum in the 2600–2900 cm^{-1} region: $2\nu_3$, $\nu_2+2\nu_3-\nu_2$ and $2\nu_1+\nu_2$ bands. J Quant Spectrosc Radiat Transfer 2012;113:500–17.
[41] Ahonen T, Karhu P, Horneman V-M. An optimized White-type gas cell for the Bruker IFS 120 high resolution FTIR spectrometer. In: Abstracts. Fifteenth colloquium on high resolution molecular spectroscopy, Glasgow, Scotland, 1997 ⟨http://physics.oulu~fi/irspe/Sivut/cell40-2002.pdf⟩.
[42] Ahonen T, Alanko S, Horneman V-M, Koivusaari M, Paso R, Tolonen A-M, et al. A long path cell for the Fourier spectrometer Bruker IFS 120 HR: application to the weak $\nu_1+\nu_2$ and $3\nu_2$ bands of carbon disulfide. J Mol Spectrosc 1997;181:279–86.
[43] V.-M. Horneman, Acta Univ. Oulu 1992;A239:1–127.
[44] Horneman V-M. Improved wave-number tables of the carbonyl sulfide ν_2 and $2\nu_2$ bands and guides for accurate measurement. J Opt Soc Am B 2004;21:1050–64.
[45] Ulenikov ON, Tolchenov RN, Koivusaari M, Alanko S, Anttila R. High-resolution fourier transform spectra of CH_2D_2: pentade of the lowest interacting vibrational bands $\nu_4(A_1)$, $\nu_7(B_1)$, $\nu_9(B_2)$, $\nu_5(A_2)$, and $\nu_3(A_1)$. J Mol Spectrosc 1994;167:109–30.
[46] Wang XH, Ulenikov ON, Onopenko GA, Bekhtereva ES, He SG, Hu SM, et al. High resolution study of the first hexad of D_2O. J Mol Spectrosc 2000;200:25–33.
[47] Ulenikov ON, Bekhtereva ES, Albert S, Bauerecker S, Hollenstein H, Quack M. High-resolution near infrared spectroscopy and vibrational dynamics of dideuteromethane (CH_2D_2). J Phys Chem A 2009;113:2218–31.
[48] Ulenikov ON, Bekhtereva ES, Alanko S, Horneman VM, Gromova OV, Leroy C. On the high resolution spectroscopy and intramolecular potential function of SO_2. J Mol Spectrosc 2009;257:137–56.
[49] Papousek D, Aliev MR. Molecular vibrational–rotational spectra. Amsterdam: Elsevier; 1982.
[50] Ulenikov ON, Hirota E, Akiyama M, Alanko S, Koivusaari M, Anttila R, et al. The high-resolution Fourier transform spectrum of dideuterated methane CH_2D_2 in the region between 1900 and 2400 cm^{-1}. J Mol Spectrosc 1996;180:423–32.

Please cite this article as: Ulenikov ON, et al. Re-analysis of the (100), (001), and (020) rotational structure of SO_2 on the basis of high resolution FTIR spectra. J Quant Spectrosc Radiat Transfer (2013), http://dx.doi.org/10.1016/j.jqsrt.2013.04.011